

Preliminary hydrodynamic assessments of a new hybrid wind wave energy conversion concept

Allan C de Oliveira*

Petrobras R&D Center, Petrobras, Av Horacio de Macedo, 950, Cidade Universitaria, Brazil

(Received November 2, 2022, Revised January 26, 2023, Accepted January 28, 2023)

Abstract. Decarbonization and energy transition can be considered as a main concern even for the oil industry. One of the initiatives to reduce emissions under studies considers the use of renewable energy as a complimentary supply of electric energy of the production platforms. Wind energy has a higher TRL (Technology Readiness Level) than other types of energy converters and has been considered in these studies. However, other types of renewable energy have potential to be used and hybrid concepts considering wind platforms can help to push the technological development of other types of energy converters and improve their efficiency. In this article, a preliminary hydrodynamic assessment of a new concept of hybrid wind and wave energy conversion platform was performed, in order to evaluate the potential of wave power extraction. A multiple OWCs (Oscillating Water Column) WEC (Wave Energy Converter) design was adopted for the analysis and some simplifications were adopted to permit using a frequency domain approach to evaluate the mean wave power estimation for the location. Other strategies were used in the OWC design to create resonance in the sea energy range to try to maximize the potential power to be extracted, with good results.

Keywords: energy; hydrodynamics; wave; WEC; wind

1. Introduction

Renewable energy utilization has been growing strongly in the last years and there are perspectives of huge growing until 2050, especially for wind energy, as reported by IRENA (2019). The pressure of the society for clean energy solutions and the technological developments in this area are reducing the economical gap between renewable and fossil energy solutions. Even for the oil industry, companies are pushed to reduce their carbon footprint and improve the sustainability of their operations to keep their competitiveness. In order to “decarbonize” as much as possible the oil production, several initiatives are being studied to reduce carbon emissions, as, for instance, the use of renewable energy to support part of the electrical power demand of the production units and the use of renewable energy to power subsea equipment. The deep and ultra-deep water oil production also brings an extra challenge of using those technologies in much higher water depths than they are being used.

Considering the renewable sources, the wind energy can be considered the readiest to be implemented in offshore ultra-deep water oil fields. Some initiatives are being studied in this field,

*Corresponding author, D.Sc., E-mail: allan_carre@petrobras.com.br

as, for instance, the studies sponsored by Equinor for the Tampen field development and seems to be a feasible way to reduce emissions minimizing the economical impacts on the production costs. Besides Equinor, other players in oil market are also investing in wind energy technology, and it may be observed a quick transition of the wind farm to deeper waters in the next years. Some wind farm scenarios include energy generation for subsea processing and also electrical hubs for distribution among floating production platforms. Although wind energy presents the greatest TRL (Technology Readiness Level) to be applied offshore, some engineering problems still remains to overcome, as increasing of mooring weights for the floater design, safety ship operational procedures and the electrical energy distribution for offshore platforms in deep waters.

Considering also the energy potential of the environment, its known that wave energy has approximately 10 to 30 times more energy density per square meter than the wind energy according to Tomalsquim (2016). Considering more specifically the Brazilian scenario, another point of attention is that the most wind powerful areas for wind energy extraction are placed in the northeast region, while the most powerful wave energy extraction areas are placed in the south and southeast areas, according to Tolmasquim (2016), in the same area where the most productive oil exploration areas are placed, indicating that the use of wind energy for electrify oil production equipment could not be as efficient as the use for people consuming in a more wind powerful area.

Although wave energy presents a greater energy potential to be used in the oil production areas, the lack of technology readiness, the low efficient of the conversion devices and consequently, the high cost per kW of the available solutions still a huge technological challenge to overcome. A possible way to explore the higher potential of wave energy decreasing the cost per energy of this technology would be the design of hybrid renewable energy conversions concepts, which means a platform capable to support more energy conversion devices (wind, wave, solar, etc.). this type of concept could also support a bank of batteries to reduce the system intermittency, improving the quality of the energy deployed.

Some types of hybrid wind and wave energy conversion concepts are being developed by different companies, as the designs of Floating Power plant, W2POWER, Wave Star As, Marine Power System and others (See, for instance, Anton *et al.* (2021) and Pérez-Collazo *et al.* (2015)), but in this paper a concept developed by PETROBRAS will be assessed. This concept uses the OWC (Oscillating Water Column) as a wave energy converter device, and it is in the preliminary feasibility studies. The aim goal of this study is assessing the potential of energy extraction that the proposed assembly is capable to reach, focused in the hydrodynamic assessments

2. Syrinx concept

According to Greaves and Iglesias (2018), OWCs “appears to be one of the most successful” technologies for wave extraction, with some different full-scale prototypes. The system consists of an air chamber under the wave action. Inside the chamber, the water oscillates and this oscillation can be used to move an equipment to convert this energy into electric energy. In the most common arrangement, the chamber usually has a cross section reduction at the top, and a wells turbine in the top of the chamber, to convert the air movement induced by the water column oscillation inside the chamber into rotation to an electric generator, as can be observed in the Fig. 1.

In order to discuss the physics of the system, Fig. 2 present a more simplified version of the system shown in Figure 1, considering a cylindrical OWC with constant Diameter D .

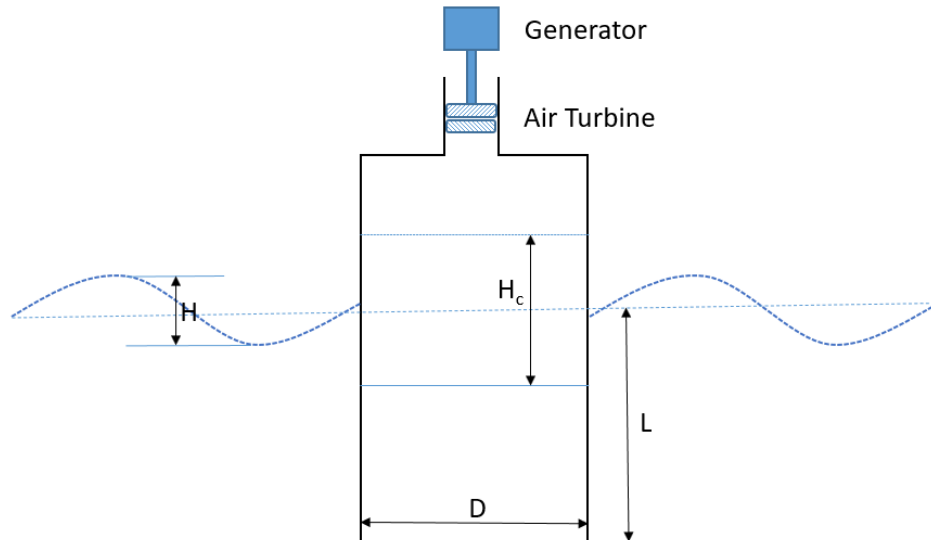


Fig. 1 Sketch of a usual design of an Oscillating Water Column for Wave Energy Conversion

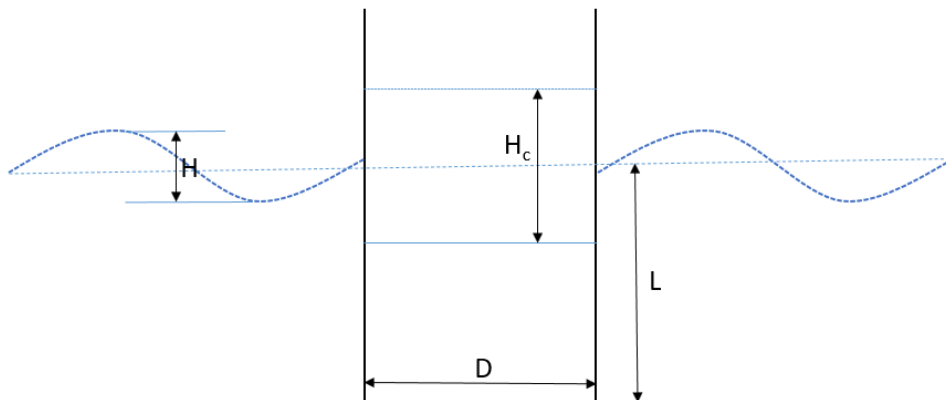


Fig. 2 Sketch of an Oscillating Water Column

Where:

H : Wave height

H_c : Wave height inside the chamber.

D : Chamber diameter.

L : Chamber Draft

As can be observed in Figs. 1 and 2, the wave heights inside the chamber were represented greater than the wave height, and it can be observed depending on the relations among the wave period T , chamber diameter D and chamber draft L . This type of resonance was usually observed in moonpools of drilling ships and several studies were performed in order to avoid this phenomenon in this kind of unit. Fukuda (1977), Evans (1978) and Lighthill (1979) are examples of studies that have

investigated that correlation among these parameters and presented the relation described in Eq. (1). For WECs, this phenomenon was studied in Jin *et al.* (2020), using a time domain approach.

$$\omega_n = \sqrt{\frac{g}{L+L_a}} \quad (1)$$

Where:

ω_n : Natural frequency of the oscillating water motion inside the chamber (rad/s)

g : Gravity acceleration (m/s²)

L_a : Additional Length (m), to represent added mass effects.

Fukuda (1977) also proposes an empirical formulation for a moonpool with constant transversal area S described in Eq. (2)

$$L_a = 0.410\sqrt{S} \quad (2)$$

Where:

S : Moonpool transversal area, or $(\pi.D^2)/4$ for a cylinder.

Silva (2009), based on a mathematical model proposes a slightly correction on Fukuda (1977) expression for cylinders, described in Eq. (3)

$$L_a = 0.479\sqrt{S} \cong 0.849R \quad (3)$$

Where:

R : Cylinder Radius, or $D/2$.

Model the resonance accurately using numerical tools may be challenging due to the nonlinear effects present on the phenomenon. Koo and Kim (2012) and Kim *et al.* (2015) are examples of studies considering time domain nonlinear model based on potential theory to predict wave elevation accurately for 2D scenarios. The use of a CFD (Computational Fluid Dynamics) is also a possibility to assess the wave elevation. Perform a frequency domain analysis, as proposed in this article, allows evaluate quickly several sea states in comparison with time domain or CFD solutions, however, it becomes necessary use simplifications and linearization in modeling to deal with these effects.

In order to understand better the relation among H , H_c and wave frequency, a single DoF (Degree of Freedom) spring-mass damped system simplification might be used as an example. Considering ω_n the resonance frequency of the chamber and also considering linear dependency between wave amplitude and wave forces, it might be possible to approximate the relation between H and H_c by the formula described in Eq. (4), very common in dynamic books (for instance, see RAO (1993)).

$$\frac{H_c}{H} \propto \frac{1}{\sqrt{\left[1 - \left(\frac{\omega}{\omega_n}\right)^2\right]^2 + \left[2\xi\left(\frac{\omega}{\omega_n}\right)\right]^2}} \quad (4)$$

The Eq. (4) to be implemented also depends on damping assumptions. As an example, considering a damping ratio (ξ) of 0.148 we can obtain the transfer curve (Response Amplitude Operator – RAO) shown in the Fig. 3(a). Applying this RAO to a JONSWAP sea spectrum of unitary significant height (H_s) and peak frequency slightly different from Moonpool resonance, it was obtained the Fig. 3(b).

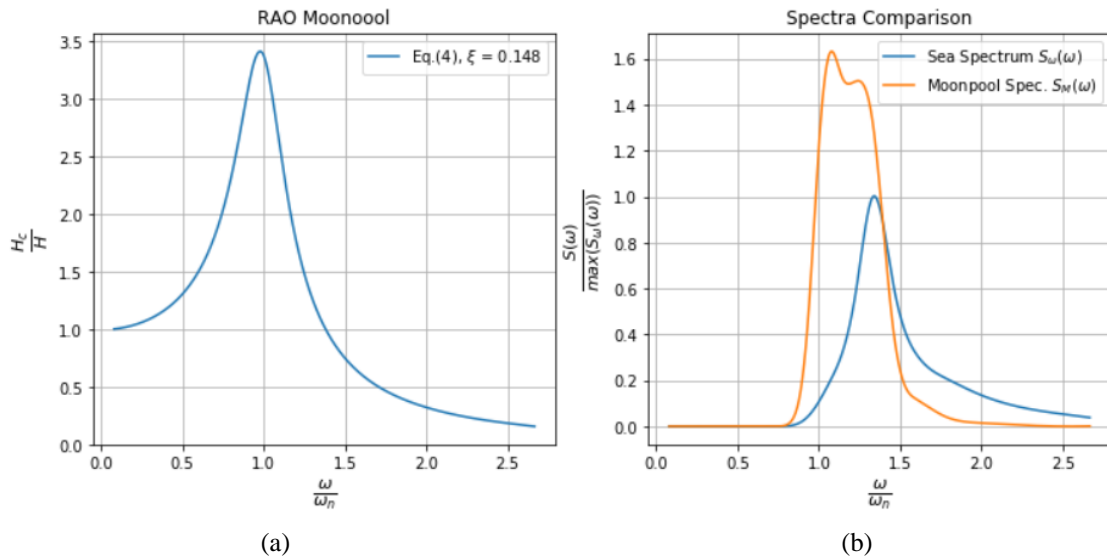


Fig. 3 (a) Example of Eq. (4) application, considering damping ratio of 0.148 and (b) Comparison of spectra considering resonance effects inside the moonpool

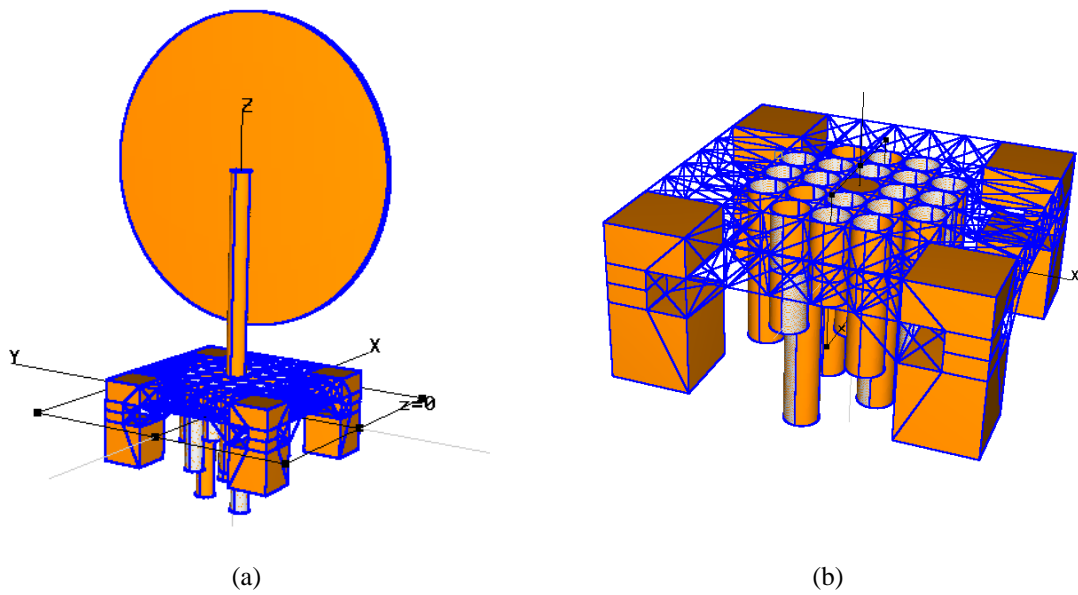


Fig. 4 Sketch of a combined wind-wave energy conversion platform. (a) Overall view and (b) Detail of wave conversion part and platform hull

As shown in the previous figure, even considering a sea spectrum slightly out of the moonpool resonance, some amplification of the wave energy inside the moonpool was achieved. In an offshore environment, wave distribution seems to be more spread along different peak periods, and because of that, a multi-column arrangement covering a wider range of periods could be useful to increase

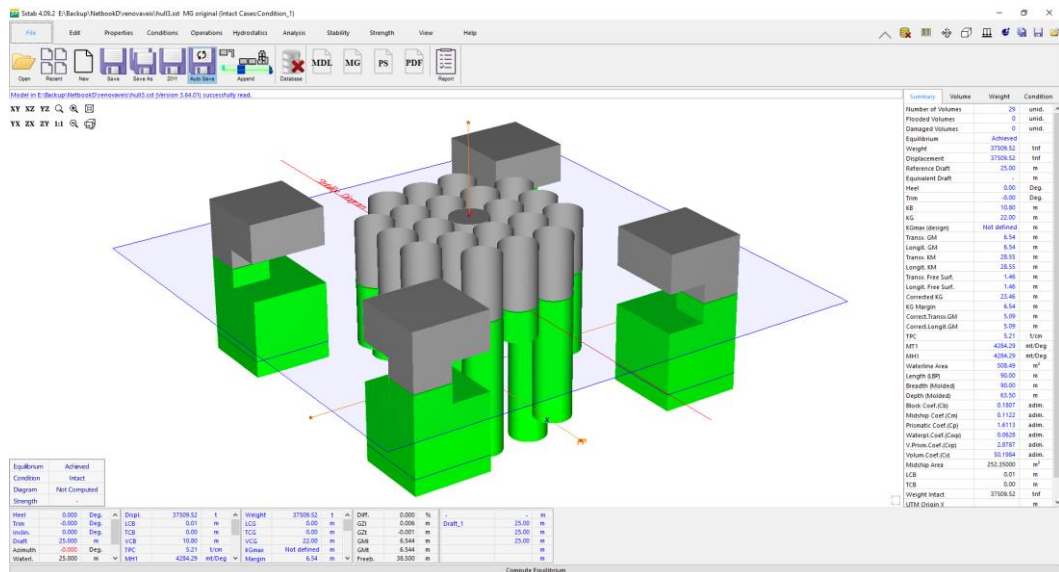


Fig. 5 PETROBRAS In House Stability Software showing the static stability model of the concept

the power recovering of the waves and reduce the intermittency of the renewable energy, specially if the wave energy conversion device is combined with offshore wind energy infrastructure (see, for instance Pérez-Collazo *et al.* (2015)). In order to test this hypothesis, a conceptual model of a combined wind-wave extraction was created for some tests. A sketch of this concept design was shown in Fig. 4.

Some preliminary analyses were performed to guarantee the static stability of the concept, as shown in Figure 5. These studies considers a wind turbine of 10 MW capability for stability checking. Another design decision applied to this concept was keeping the natural heave period of the hull over 20 seconds. This decision was taken to avoid two aspects. The first one was avoid resonances of the heave motions of the unit at the site. Usually, conventional hull forms used to support offshore wind turbines have heave natural periods close to the range between 15 and 17 seconds, inside the sea energy range for the extreme waves from the site (Lima *et al.* 2011). The second aspect was avoid coincidences between the heave motion resonance and the cylinder's resonance in order to study a wider range of Oscillating Water Column (OWC) resonance periods (up to 14.5 seconds). This kind of coincidence could create a coupling between the motion of the hull and the motion of the water inside the cylinder.

These constraints were imposed in order to avoid interferences among hull resonances, sea energy and the OWC resonances, to simplify the analysis. Because of them, the hull displacement of this concept (37,000 tons) has become bigger than an usual wind energy typical hull (17,000 tons). Besides that, the hull also presents a smaller water plane area, as can be observed in Fig. 5. For this preliminary design, no optimization study was performed to minimize the size of the platform. To evaluate a real application of this concept, this kind of study on the hull form is highly acknowledged.

The design of the multi-column arrangement, with different lengths of the submerged parts, reminds a musician instrument called Pan's flute or Pan's pipe (at least for the designer), and, because of that, the concept was called SYRINX (SYstem of Resonance Induced for eNErgy eXtraction) concept. According to Wikipedia (2021), Syrinx was a nymph pursued by the god Pan.

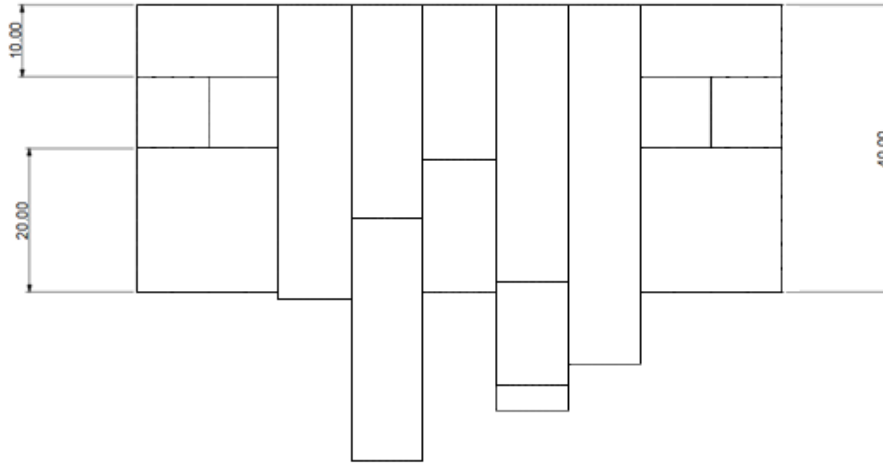


Fig. 6 Front view of the Hull. Dimensions in Meters

Table 1 Hull main characteristics

	Prototype
Length	90.0 m
Breadth	90.0 m
Depth*	40.0 m
Draft*	25.0 m
Column length	20.0 m
Neck length	10.0 m
Cylinder Diam. (internal)	9.50 m
Cylinder Diam. (External)	10.0 m
VCG*	22.0 m
Displacement	37,509 ton

To escape from him, she asked for the river nymph’s help and was transformed into hollow water reeds.

3. Preliminary hydrodynamic assessments

As previously mentioned, one constraint of the design was natural periods over the resonance periods of the cylinders, in order to simplify the analyses. In order to assure that, a hydrodynamic simplified model was built and natural periods were computed using WAMIT[®] (MIT (2001)) software. The hull dimensions and characteristics are shown in the Figs. 6, 7 and Table 1.

Based on these dimensions, a WAMIT[®] model was built, as shown in Fig. 8. The idea of the WAMIT[®] model was check the natural periods over the cylinder resonance periods, because the

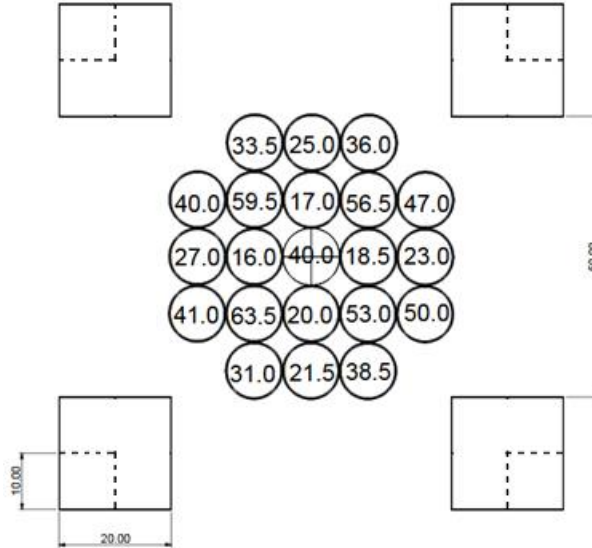


Fig. 7 Upper view of the Hull. Dimensions in Meters. Cylinders depths (inside the cylinders) are measured from the top of the model

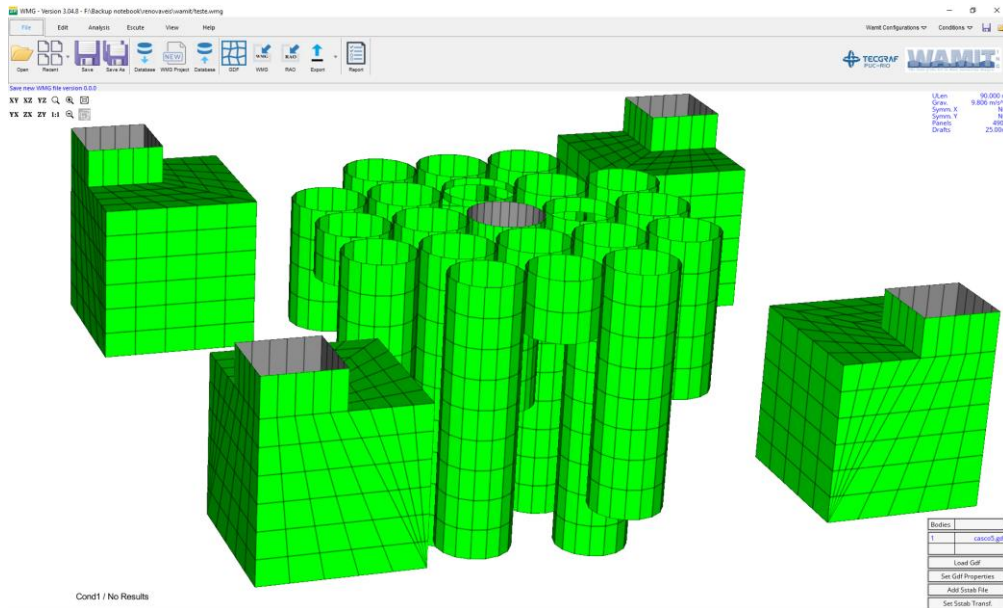


Fig. 8 PETROBRAS In House Software for WAMIT® pre and pos processing showing the mesh of the concept, with 4909 panels

internal resonance inside the cylinders is strongly associated with viscosity, in such way that BEM (Boundary Element Methods) based on Laplace Equations like WAMIT® have difficulties to capture well the behavior inside the moonpool.

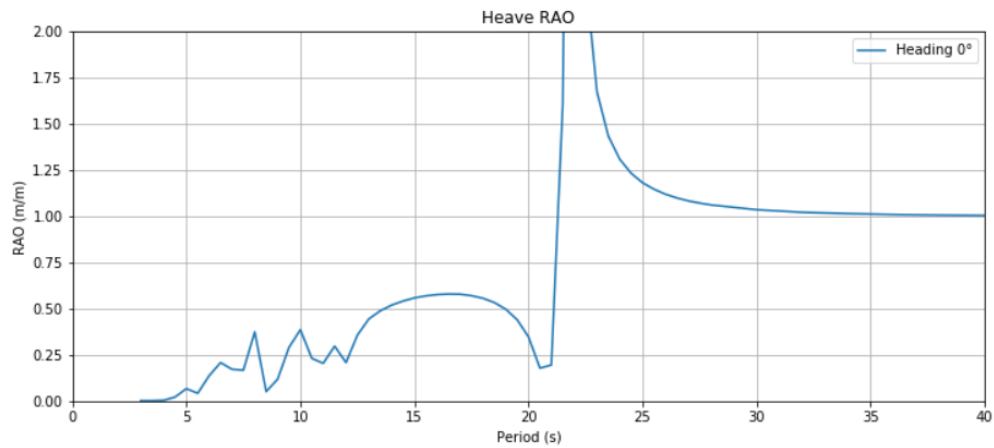


Fig. 9 Heave RAO, with noisy behavior caused by cylinders resonances without damping

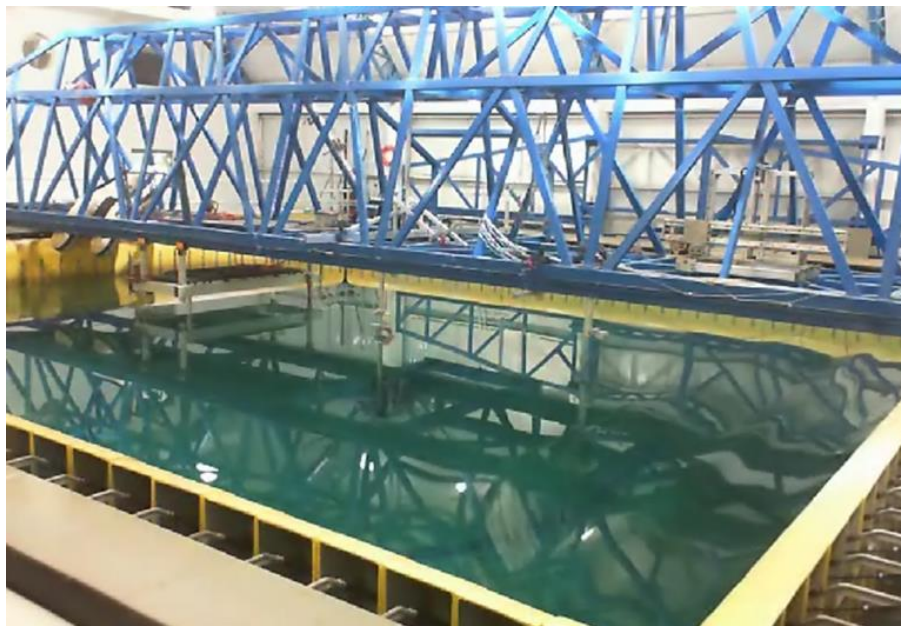


Fig. 10 Numerical Offshore Tank Wave basin facility

A WAMIT® model like the one shown in Fig. 8 might have, at least, three potential sources of numerical problems: The small thickness of the cylinders, the small distance among them and their openings, which are, by design, resonant for some determined frequencies.

Thickness can be treated using a model thicker than in reality, using a thickness big enough to avoid numerical problems but small enough to have negligible impact in the hydrostatic stiffness.

The other sources, however, are more difficult to treat and usually requires a comprehensive model test to support modeling. The gaps among the cylinders can induce some kind of wave mode,

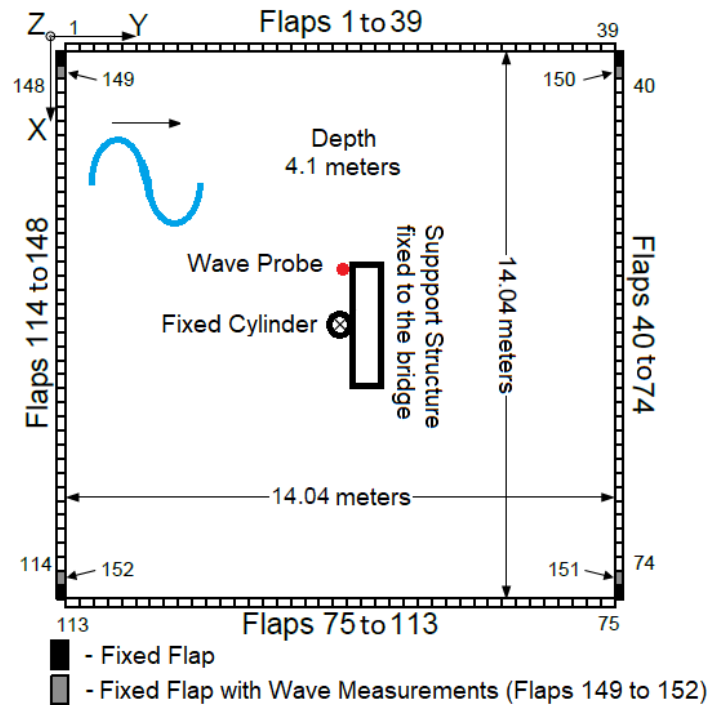


Fig. 11 Simplified model test set up assembly, considering an isolated cylinder varying depth

as well as a piston mode is expected inside the OWC. Both effects may introduce numerical instabilities and introduce error in the wave surface elevation assessment.

There are several references in literature which discuss how improve BEM hydrodynamic models (using WAMIT[®], HYDROSTAR[®] and AQWA[®] software) to describe the behavior of an OWC inside a hull model (see for instance Torres (2007) and Costa (2019)), but, in general, the application of these methods requires a model test to calibrate the damping of the fluid inside the OWC.

The Fig. 9 shows the Heave RAO obtained in WAMIT[®] for the model shown in Fig. 8. Despite the sources of problems described earlier, it is possible to observe the Heave Natural Period of the hull around 22 seconds and a huge noise in the cylinder resonance range, which is a good indicative that Fukuda (1977)/Silva (2009) formulations to design the cylinder depths has produced the expected results. The numerical results inside the OWC, however, are strongly affected by those problems and the investigation and modeling of these behavior still a research in progress.

Because of those complexities, a simplified numerical model was chosen as first approach to represent the behavior of the OWCs inside the cylinders. To support this simplified numerical approach, an also simplified experimental assessment was chosen to evaluate the behavior of the water inside the cylinders.

To follow this way to assess the internal oscillation of the water column inside the cylinders, it was decided to use the model described in Eq. (4), with the damping ratio calibrated using simplified model tests. The simplified model test considers an isolated cylinder varying depth to adjust the resonance period while a wave probe measures the internal amplitude of the oscillating water column

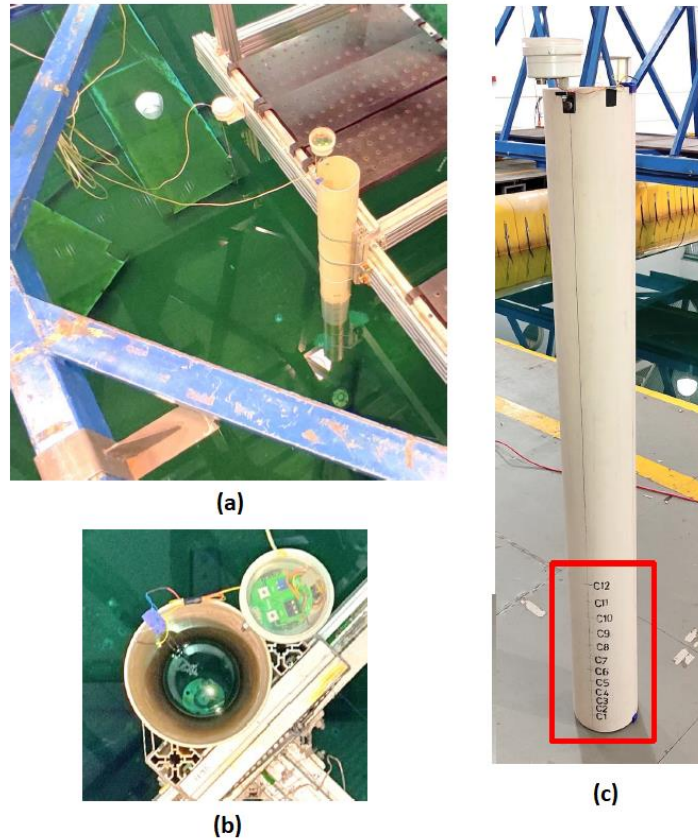


Fig. 12 Details of the model test in the facility: (a) Cylinder and wave probe assembly, (b) Water level measurement inside the cylinder and (c) Draft marks on the cylinder to be tested

inside the moonpool. The tests were performed at the wave basin of the Numerical Offshore Tank (TPN – Tanque de Provas Numérico) at São Paulo University (Fig. 10). Despite the name, the laboratory has a small physical facility usually used to calibrate their numerical models used in numerical simulators or provide small and prospective tests.

The wave basin has 14 m of length and breadth, and 4 meters of depth, and the model set up in the wave basin was mounted according to the Fig. 11.

The tests were performed using a scale factor of 1:67 using a commercial pipe fixed at a support structure fixed at the bridge of the tank, as shown in Fig. 12(a). A wave probe was positioned in the same structure to measure the wave acting on the cylinder, as shown in the same figure. A wave probe was also installed inside the cylinder, as shown in Fig. 12(b), to measure the wave elevation and how resonance affects these elevations. Concerning the waves, regular, white noise and an irregular with significant height of 2 meters (prototype scale) were tested for 12 submerged lengths, as shown in Fig. 12(c).

The wave periods of the regular wave and the peak period of the irregular wave was set up to be in resonance with the cylinder resonance period. The H_s chosen for the irregular wave was the mean value expected for location, 2 meters in the prototype scale. Fig. 13 shows an example of the response obtained in the facility. Due to the limitations of the facility to the scale selected, it was not

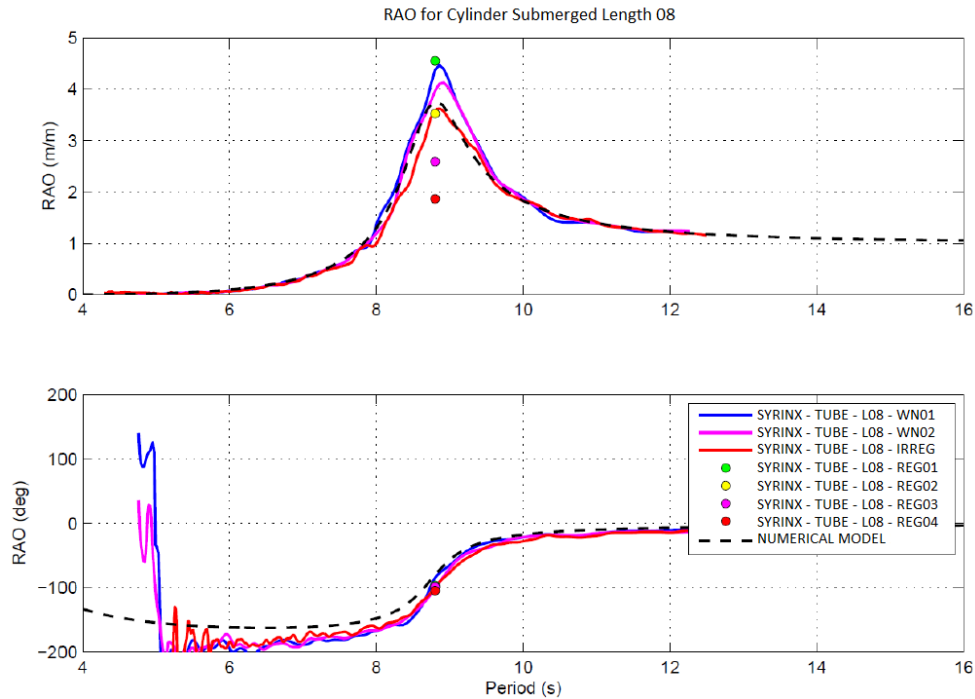


Fig. 13 Example of result generated by the facility. In this example, 2 white noise waves (constant energy by frequency – WN01 & WN02), an irregular wave (IRREG – H_s 2.0 meter and T_p = Resonance period of the cylinder), and 4 regular waves (REG01, 02, 03 and 04)

Table 2 Hull main characteristics. Damping ratio obtained by the numerical model calibration

Lengths	T moonpool (s)	RAO (m/m)	Damping ratio (ξ)
L01	5	1.18	0.48
L02	5.5	1.54	0.35
L03	6	1.82	0.29
L04	6.6	2.71	0.185
L05	7.2	3.03	0.166
L06	7.7	3.16	0.16
L07	8.3	3.4	0.149
L08	8.8	3.76	0.135
L09	9.4	4.4	0.115
L10	9.9	4.3	0.118
L11	10.4	4.7	0.107
L12	11	4.53	0.11

possible to run irregular waves for the all the range of periods of the test, and the irregular wave was used as a guide to select regular the best wave height to be used to calibrate damping among 4 different wave heights tested. Therefore, the numerical model was adjusted to the regular wave

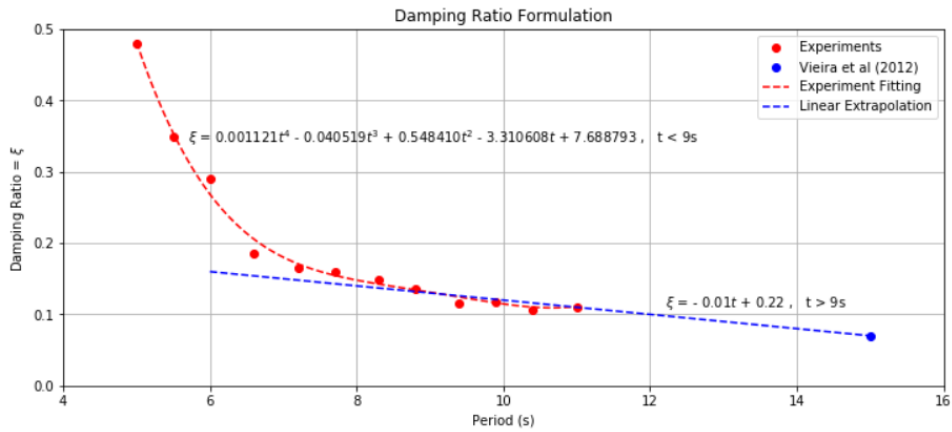


Fig. 14 Mixed (literature + experiments) damping model

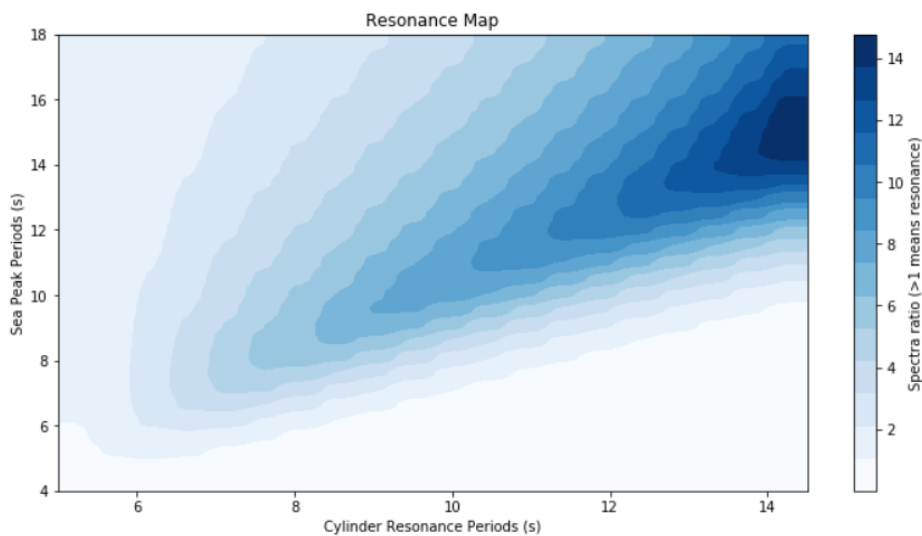


Fig. 15 Sea energy amplification mapping. White region is the non-resonance region

response at natural frequency of the water inside the cylinder. White noise waves with correspondent energy of H_s equal to 1 meter and 2 meters were also tested in order to try to extend the facility period covering, but the results were not used because they usually became less damped than the irregular wave tests, as shown in Fig. 13. Table 2 shows the calibration results for damping ratio considering damping model presented in Eqs. (4) and (20). To calibrate the damping in Table 2, the expression show in Eq. (4) to estimate damping ratio (ξ), considering $\omega = \omega_n$, and using an iterative method to vary ξ until (H_c/H) equal to the RAO peak obtained experimentally.

Due to the model scale, it was not possible to obtain the RAOs for periods over 11 seconds (prototype scale) even using regular waves. In order to estimate higher periods, it was used a reference about Monocolumn platform moonpool damping (Vieira *et al.* 2012) to estimate the

damping ratio of 0.07 for moonpool resonance period of 15 seconds. Considering a straight line from the last experimental point and the literature point it can be observed the graph shown in Fig. 14. Extending the straight line, it was decided to adopt the nonlinear formulation shown in Fig. 14 until 9 seconds of resonance moonpool period and adopt the linear model for resonance periods over 9 seconds according to the Figure. It was decided because of the oscillating behaviour presented by the experiment damping over 9.5 seconds.

Since a damping model is established, it is possible to compute, for each moonpool resonance period, the estimated RAO of the moonpool. Using this RAO it is also possible to compute the response spectrum of the moonpool for a sea of unitary significant height (H_s) as shown in Figures 3 and 4. Computing the area of these spectra, it is also possible to compute the amplification factor, i.e., the ratio between the moonpool response spectrum area and the sea spectrum area. For amplification factors above 1, it means that the moonpool amplifies the sea energy in the area inside the moonpool. Performing those calculations for different moonpool resonance periods and also for different sea peak periods, it is possible to map the situations where amplification occurs, as shown in the Fig. 15. The sea spectrum considered in Fig. 15 is a JONSWAP spectrum adapted to Brazilian measurements (Lima *et al.* 2011).

As can be observed in Figure 15, it was possible to observe a huge energy amplification zone which is an indication that would be possible use this resonance mechanism to extract more power from a site, as will be more stressed in the next section.

4. Preliminary wave power assessments

From literature (for instance, see Greaves and Iglesias 2018), the wave energy can be assessed computing the sum of kinetic and potential energy of the waves. The kinetic energy, E_k for a 1-meter width of wave crest and one wavelength (L) can be written as

$$E_k = \int_x^{x+L} \int_{-d}^0 \rho \frac{(u^2+v^2)}{2} dz dx \quad (5)$$

Where

$$u(x, z, t) = \frac{H}{2} \omega \frac{\cosh[k(d+z)]}{\sinh(kd)} \cos(kx - \omega t + \theta) \quad (6)$$

$$v(x, z, t) = \frac{H}{2} \omega \frac{\sinh[k(d+z)]}{\sinh(kd)} \sin(kx - \omega t + \theta) \quad (7)$$

$$k = \frac{2\pi}{L} \quad (8)$$

The potential energy E_p can be written as

$$E_p = \int_x^{x+L} \rho g \left[\frac{(\eta+d)^2}{2} - \frac{d^2}{2} \right] dx \quad (9)$$

$$\eta = \frac{H}{2} \cos(kx - \omega t + \theta) \quad (10)$$

Solving these integrals, it can be found kinetic, potential and total energies, which are equal to

$$E_k = E_p = \frac{1}{16} \rho g H^2 L \therefore E = E_k + E_p = \frac{1}{8} \rho g H^2 L \quad (11)$$

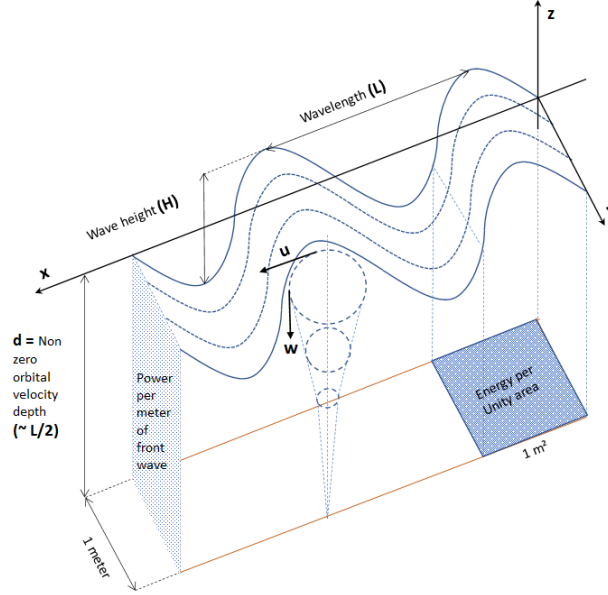


Fig. 16 Wave definitions for wave energy/power assessments

It is possible to define the average energy per unit surface area dividing the energy by wavelength by the wavelength.

$$\bar{E} = \frac{E}{L} = \frac{1}{8} \rho g H^2 \quad (12)$$

The wave power is usually defined as the product of the force acting on a vertical plane normal to the wave propagation direction, as shown in Fig. 16. For a regular wave, the power can be computed by the average energy per unity area multiplies by the group velocity of the wave (C_g). Developing this expression, it can be found that the power in regular waves can be approximated by the following expression

$$\bar{P} = \bar{E} C_g \approx H^2 T \quad (13)$$

For irregular waves with Significant Height H_s , the power is given by the Eq. (14) (Andrioni *et al.* 2013)

$$P = \rho g \int_0^\infty C_g(f) S_w(f) df = \frac{1}{2} H_s^2 T_e \quad (14)$$

Where

$$T_e = \frac{m_{-1}}{m_0} \therefore m_n = \int_0^\infty f^n S_w(f) df \quad (15)$$

T_e can be also approximated to $0.9 T_p$. This approach computes the wave energy by a meter of wave front. Although this approach is the most common to assess power from waves, due to the characteristics of the Syrinx concept, the assessment will consider the average energy per unit surface area to perform the comparisons about the energy that can be recovered by the system. For irregular waves, the average energy per unit surface area can be written as

$$\bar{E} = \frac{E}{L} = \frac{1}{8} \rho g H_S^2 \quad (16)$$

Another limitation of the concept is basically only using the potential part of the wave energy to capture energy, so, the potential part of the average energy per unit surface are given by

$$\bar{E}_p = \frac{E_p}{L} = \frac{1}{16} \rho g H_S^2 = \frac{1}{16} \rho g (4\sqrt{m_0})^2 = \rho g m_0 \quad (17)$$

Where m_0 is the sea spectrum area. This simplification allows use a frequency domain approach to assess the amount of energy available on a site area. Applying this approach in a Brazilian area, which wave scatter are shown in the Fig. 17, it is possible to assess the mean potential energy available for this area. It is also important to remind that the potential energy is a maximum of energy that can be theoretically recovered from the sea. The real energy recovered would depend also on the efficiency of the wave energy conversion mechanism used.

Applying the Eq. (17) to the sea states presented in the Fig. 17, It was found a mean energy of **3.933 kJ/m²**. Applying this mean energy to the area of the Syrxin cylinders (20 cylinders of 9.5 meters of diameter) a system without any amplification could generate a potential mean energy of **5.57 MJ**.

To assess the mean power of the area, Eq. (17) needs to be multiplied by a group velocity which is defined for regular waves, and can be written as a frequency function $C_g(f)$. Remembering Eq. (15), m_0 is the area of the spectrum curve, or the integral of $S_w(f)$. Integrating the product $C_g(f) * S_w(f)$ allows to assess the power as defined in Eq. (14) for each sea state. Applying tis formulation to the same sea states, it was found a mean power of **496.4 kW/m** (remarking that the real power value must consider the conversion efficiency and would be significantly lower than that). For a very gross estimation, multiplying the cylinder diameter for this mean power, it was found a potential power of **4.715 MW** for a system without wave amplifications inside the cylinders.

To evaluate the power achieved by the Synrix concept, it is also necessary to consider the amplification factors shown in the Fig. 15 to each sea state in Fig. 17 when computing the spectrum area. In this case, the Eq. (17) is computed for each system cylinder, considering the specific amplification factor (α_i), as shown in the Eq. (18).

$$\bar{E}_{p_i} = \frac{E_{p_i}}{L} = \frac{1}{16} \rho g H_S^2 \alpha_i(T_{n_i}, T) = \frac{1}{16} \rho g (4\sqrt{m_0})^2 \alpha_i(T_{n_i}, T) = \rho g m_0 \alpha_i(T_{n_i}, T) \quad (18)$$

The amplification is the area ratio between the response spectrum of the moonpool for a given sea state and the sea state itself, as shown in Eq. (19), and it is function of the resonance period of the cylinder (T_{n_i}) and the peak period of the irregular sea (T).

$$\alpha_i(T_{n_i}, T) = \frac{\int_0^\infty RAO^2(T_{n_i}, \omega, \xi) S_w(\omega) d\omega}{\int_0^\infty S_w(\omega) d\omega} \quad (19)$$

The RAO is computed using the expression shown in Eq. (4)

$$RAO(T_{n_i}, \omega, \xi) = \frac{1}{\sqrt{[1 - (\omega/\omega_{n_i})^2]^2 + [2\xi(\omega/\omega_{n_i})]^2}} \quad (20)$$

Where $\omega_{n_i} = \frac{2\pi}{T_{n_i}}$ and ξ is given by the formulation shown in Fig. 14 (replacing t by T_{n_i}).

Since the cylinders have the same diameter, the average energy per unit surface is given by

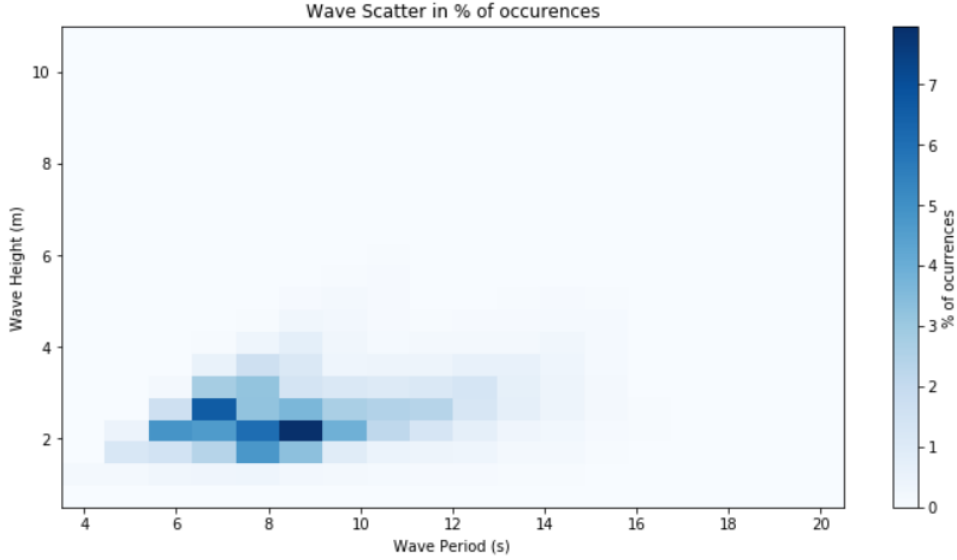


Fig. 17 Sea occurrence probabilities for a Brazilian area (Lima *et al.* 2011)

$$\bar{E}_p = \sum_{i=1}^{20} \bar{E}_{p_i} \quad (21)$$

And the potential wave energy for a given sea state is obtained by

$$E = \frac{\pi}{4} D_{cyl}^2 \bar{E}_p \quad (22)$$

Where D_{cyl} is the diameter of the cylinder. Applying Eq. (22) to the sea states presented in Fig. 15, it was found a mean energy of **13.180 kJ/m²**, an increase of **235%** in relation of a non-resonant system. Considering the area of the concept, the mean potential energy achieved was **18.68 MJ**. In a similar way, to compute power, the amplification factor in Eq. (19) needs to be modified to include the group velocity, as shown in Eqs. (23) and (24)

$$\bar{P}_{p_i} = \frac{E_{p_i}}{L} \cdot c_g = \frac{1}{16} \rho g H_S^2 \beta_i(T_{n_i}, T) = \frac{1}{16} \rho g (4\sqrt{m_0})^2 \beta_i(T_{n_i}, T) = \rho g m_0 \beta_i(T_{n_i}, T) \quad (23)$$

$$\beta_i(T_{n_i}, T) = \frac{\int_0^\infty RAO^2(T_{n_i}, \omega, \xi) \cdot c_g(\omega) S_w(\omega) d\omega}{\int_0^\infty S_w(\omega) d\omega} \quad (24)$$

Since the cylinders have the same diameter, the average power per length is given by

$$\bar{P}_p = \sum_{i=1}^{20} \bar{P}_{p_i} \quad (25)$$

Computing the Eq. (25) for several sea states, it is possible to build a map of the wave potential power per length of the concept, as shown in Fig. 18. Combining the power data from Fig. 18 and the probabilities of occurrence shown in Fig. 17, it is also possible to compute the mean expected potential power per length for the location.

Recomputing the power considering the amplification factors, the mean power of the Synrix concept was **2.109 MW/m**, an increase of **325%** in relation of a non-resonant system. This

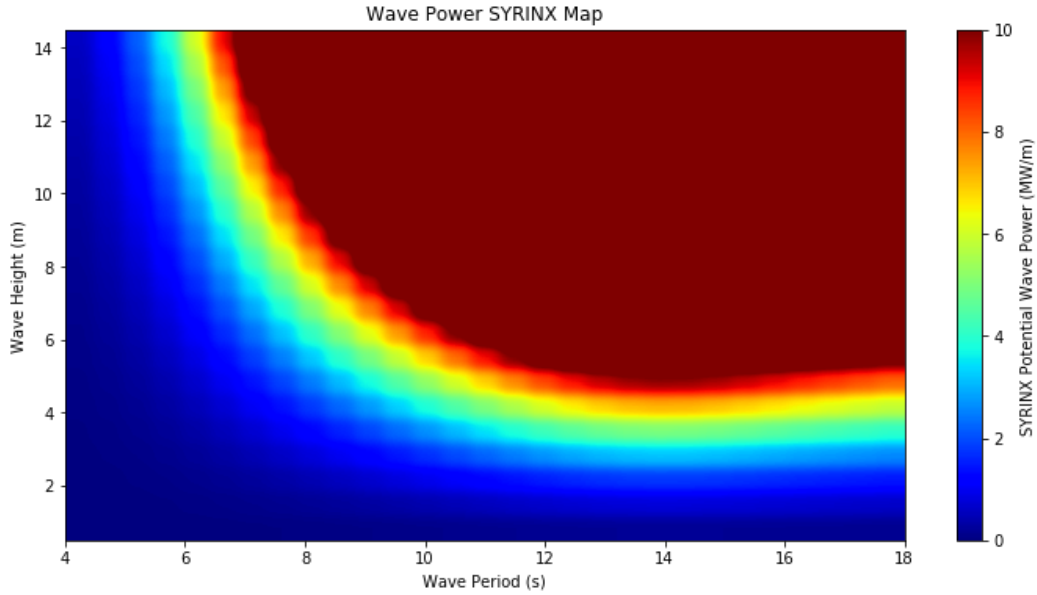


Fig. 18 Map of Expected potential power for each sea state, defined by a H_s (Wave Height) and a Peak Period (Wave Period)

amplification value for power is greater than the one achieved by the amplification energy (235%) and is related to the nonlinear behavior of the group velocity with the wave period. For a very gross estimation, the potential power for a given sea state is obtained by

$$P = D_{cyl} \bar{P}_p \quad (26)$$

Recomputing the power considering the cylinder diameter for this mean value, it was found a potential power of **20.04 MW**. Although there are very preliminary power evaluations, these values are high enough to justify complementary studies about this concept, considering hybrid wind-wave extraction energy concepts.

5. Conclusions

This article proposes a combined wave-wind energy extraction platform concept. There were performed hydrodynamic analyses in order to assess the wave energy availability for a Brazilian offshore site

As results, it was developed a concept based in Oscillating Water Column principle, considering multi-columns to increase the energy extraction and reduces the energy intermittency. Very preliminary hydrodynamic assessments were performed to check the feasibility and the capacity of the model proposed to increase the energy extracted per area. An increase of 235% was achieved in these analyses, which justifies more effort in the development of the concept, as well as, more realistic model tests to refine these numbers.

The evaluations for potential power of the area has shown an amplification even greater, of 325% in relation to a non-resonant system. This kind of result is a good insight maximize power recovery

might not be related to maximize energy amplification of the area. Once again, it is important to remark that the real power value must consider the conversion efficiency and also the uncertainties related to the simplifications used and, as a consequence, power would be significantly lower than that value found.

The hydrodynamic assessments presented in this article have assumed simplifications and linearizations, in order to use a frequency domain approach. Because of that, uncertainties are introduced in the results, and further analysis should revisit these assumptions. Despite these uncertainties, the results obtained for the potential wave energy also shows that the Synrix concept has potential to work in combined wind-wave energy extraction scenarios.

6. Future work

As mentioned before, the assessments performed to the Synrix concept were preliminary, so there are several assessments that needs to be made in order to improve the concept design.

In terms of hydrodynamic assessment, the strategy adopted so far is quite basic. To make progress, however, it is necessary strong support in model test data. The singular cylinder model used in the preliminary tests does not capture interference effects among the cylinders, like shadow effects.

Design the model test also requires more instrumentation than a regular offshore platform model test, since the behavior of each oscillating water column would be assessed, increasing the instrumentation weight in the model. Using a normal scale for offshore wave basins (1:100 – 1:70) may be challenging since the displacement of the model will be smaller compared to offshore platforms models, with smaller margins for instrumentation. Using a greater scale, however, may reduce the wave range assessed, depending on the laboratory resources. Because of that, some kind of compromise solution shall be adopted to carry on with those tests.

The tests done for this article have considered a single cylinder fixed. The next test campaign, considering this idea of compromise solution, should focus on the presence of multiple OWCs (still fixed), to understanding how grouping the cylinders should affect the results considering shadow effects and even reflection effects. Depending on the results, a free floating campaign in a greater scale should be considered.

Regarding the damping extrapolation, other types of approach with some conservative bias are possible. Considering the response inside the cylinder greater as the damping reduces, approaches that overestimates the damping would underestimate the amplification, with impact in energy and power computations, keeping a conservative bias in these estimations. In this article, another approach was implemented, using a literature reference to guide the extrapolation as one of the simplifications assumed to build a frequency domain computation algorithm. Further analysis should consider a conservative bias approach in case of not being possible investigate all frequencies experimentally.

Another hydrodynamic important aspect that needs to be addressed is the nonlinear behavior of the waves inside the cylinder (wave height was sized to the mean H_s expected for the site area) and it is important to develop the concept design and shall be addressed in the model tests. The capability of calibrate a numerical hydrodynamic model is also important to develop the system design and shall be investigated during model tests.

A good hydrodynamic model will help to use optimization techniques to determine the best cylinders configuration for each site area, considering aspects as the maximization of the energy

extraction and the minimization of the cost of the structure, for instance. Assessments about the equipment to make the energy conversion are also necessary to be addressed.

Acknowledgments

The authors would like to thank the Petrobras R&D Center for the financial support, especially Mr. Daniel Fonseca de Carvalho e Silva who made available the wave basin tests presented in this article. The TPN team responsible for the tests is also acknowledged, especially Prof. Kazuo Nishimoto, Mr. Daniel Prata Vieira and Mr. Pedro Cardozo de Mello.

References

- Antón, M., Eskilsson, C., Andersen, J., Kramer, M.B. and Thomas, S. (2021), “Floating power plant hybrid wind-wave platform: CFD simulations of the influence of chamber geometry”, *Developments in Renewable Energies Offshore*, Taylor & Francis Group, London, Great Britain.
- Costa, D.O. (2019), *Utilização de Sistema de Colunas d’Água Oscilantes no Controle de Pitch de um Casco FPSO* (Use of Oscillating Water Column System to Control the pitch Response of a FPSO Vessel), Master in Science dissertation, Federal University of Rio de Janeiro, Rio de Janeiro, Brazil. (In Portuguese).
- Evans, D. (1978), “The oscillating water column wave-energy device”, *J. Inst. Math. Appl.*, **22**(4), 423-433. <https://doi.org/10.1093/imamat/22.4.423>.
- Fukuda, K. (1977), “Behavior of water in vertical well with bottom opening of ship, and its effects on ship motion”, *J. Soc. Naval Archit. Jap.*, **141**, 107-122. <https://doi.org/10.2534/jjasnaoe1968.1977.107>.
- Greaves, D. and Iglesias, G. (2018), “Wave and tidal energy”, 1st Ed., John Wiley & Sons Ltd. Great Britain.
- IRENA (2019), *Future of wind: Deployment, investment, technology, grid integration and socio-economic aspects* (A Global Energy Transformation paper), International Renewable Energy Agency, Abu Dhabi.
- Jin, C., Kang, H., Kim, M. and Cho, I. (2020), “Performance estimation of resonance-enhanced dual-buoy wave energy converter using time-domain simulator”, *Renew. Energ.*, **160**, 1445-1457. <https://doi.org/10.1016/j.renene.2020.07.075>.
- Kim, S.J., Koo, W.C. and Kim, M.H. (2015), “Nonlinear time-domain NWT simulation for two types of a Backward Bent Duct Buoy (BBDB) compared with a 2D wave-tank experiments”, *Ocean Eng.*, **108**, 584-593. <https://doi.org/10.1016/j.oceaneng.2015.08.038>.
- Koo, W.C. and Kim, M.H. (2012), “A time-domain simulation of a oscillating water column with irregular waves”, *Ocean Syst. Eng.*, **2**(2), 147-158. I: <https://doi.org/10.12989/ose.2012.2.2.147>.
- Lighthill, J. (1979), “Two -dimensional analyses related to wave-energy extraction by submerged resonant ducts”, *J. Fluid Mech.*
- Lima, J.A.M, Ribeiro, E.O., Nunes, L.M.P. and Oliveira, M.C. (2011), “Metoccean data”, Petrobras Technical Specification, I-ET-3*26.00-1000-941-PPC-001 Revision C, Rio de Janeiro, Brazil.
- MIT (2001), “WAMIT 6.0, A Radiation, Diffraction Panel Program for Wave Body Interactions”, Cambridge: The MIT Press, Cambridge, MA, USA.
- Nader, J.R., Zhu, S.P., Cooper, P. and Stappenbelt, B. (2012), “A finite-element study of the efficiency of arrays of oscillating water column wave energy converters”, *Ocean Eng.*, **43**, 72-81. <https://doi.org/10.1016/j.oceaneng.2012.01.022>.
- Nishimoto, K., Videiro, P.M., Fucatu, C.H. Matos, V.L.F., Cueva, D.R. and Cueva, M.S. (2001), “A study of motion minimization devices of FPDSOs”, *Proceedings of the International Conference on Offshore, Mechanical and Artic Engineering, OMAE-2001*, Rio de Janeiro, Brazil.
- Pérez-Collazo, C., Greaves, D. and Iglesias, G. (2015), “A review of combined wave and offshore wind energy”, *Renew. Sust. Energ. Rev.*, **42**(2015), 141-153. <https://doi.org/10.1016/j.rser.2014.09.032>.

- RAO, S.S. (1993), “Mechanical vibrations”, Addison-Wesley.
- Silva, E.A. (2009), “Coluna de Água Oscilante Aplicada ao Controle de Movimentos de Unidades FPSO”, (Oscillating Water Column Applied to FPSO Motion Control), Naval Architecture Graduation Final Report, Federal University of Rio de Janeiro, Rio de Janeiro, Brazil. (In Portuguese).
- Sphaier, S.H., Torres, F.G.S., Masetti, I.Q., Costa, A.P. and Levi, C. (2007), “Monocolumn behavior in waves: Experimental analyses”, *Ocean Eng.*, **34**(11-12), 1724-1733. <https://doi.org/10.1016/j.oceaneng.2006.10.017>.
- Torres, F.G.S., Cueva, M.S., Nishimoto, K. and Malta, E.B. (2004), “Hydrodynamic design of a Monocolumn Platform – MONOBR, SOBENA (Brazilian Society of Naval Architects). Rio de Janeiro, Brazil.
- Torres, F.G.S. (2007), “Estudo do Moonpool como Sistema de Minimização de Movimento em uma Plataforma do Tipo Monocoluna” (Moonpool Studies as Motion Minimization Mechanism in Monocolumn Platforms), Master in Science Dissertation, São Paulo University, São Paulo, Brazil. (In Portuguese).
- Tolmasquim, M.T. (2016), “Energia Renovável: Hidráulica, Biomassa, Eólica, Solar, Oceânica”, (Renewable Energy: Hydraulics, Biomass, Wind, Sun and Waves) EPE (Brazilian Energy Research Company), Rio de Janeiro, Brazil. (In Portuguese).
- Vieira, D.P., Watai, R.A., Fajarra, A.L.C., Malta, E.B., Gonçalves, R.T., Nishimoto, K. and Oliveira, A.C. (2012), “MPSO design: Part I – wave excitation forces and moments”, *Proceedings of the International Conference on Offshore, Mechanical and Arctic Engineering, OMAE-2012*, Rio de Janeiro, Brazil.
- Wikipedia (2021), “Syrinx”, available at URL: <https://en.wikipedia.org/wiki/Syrinx> (Accessed: 1st August 2021).